

**Metal-insulator transition in boron-ion-implanted diamond**T. Tshepe,<sup>1</sup> C. Kasl,<sup>1</sup> J. F. Prins,<sup>2</sup> and M. J. R. Hoch<sup>1,\*</sup><sup>1</sup>*School of Physics and Materials Physics Research Institute, University of the Witwatersrand, P.O. WITS, 2050, South Africa*<sup>2</sup>*Schonland Centre for Nuclear Sciences, University of the Witwatersrand, P.O. WITS, 2050, South Africa*

(Received 17 August 2004; revised manuscript received 27 September 2004; published 8 December 2004)

We have observed the metal-insulator transition in single crystal, high-purity type-IIa diamond which has been implanted at 77 K with boron ions in multiple steps and annealed at high temperatures between implants. Electrical conductivity measurements made at temperatures in the range 1.5–300 K have shown that, for boron concentrations below the critical concentration  $n_c$  which we estimate as  $3.9 \times 10^{21} \text{ cm}^{-3}$ , Efros-Shklovskii hopping conduction occurs at sufficiently low temperatures. At the highest concentrations, just-metallic behavior is found, with the low-temperature conductivity governed by the relation  $\sigma(T) = \sigma(0) + bT^m$ . The conductivity critical exponent  $\mu$  is estimated to be 1.7, with a fairly large uncertainty because of the limited number of concentrations on the metallic side of the transition. The high  $\mu$  value found for this wide bandgap, uncompensated  $p$ -type system contrasts with the value  $\mu \approx \frac{1}{2}$  reported for  $p$ -type Si and other uncompensated semiconductors.

DOI: 10.1103/PhysRevB.70.245107

PACS number(s): 71.30.+h, 72.20.Ee, 73.23.-b

**INTRODUCTION**

The metal-insulator (MI) transition is an important topic in condensed matter physics. A variety of systems have been studied, with considerable emphasis on doped semiconductors such as silicon and germanium.<sup>1–5</sup> Very little work related to the MI transition has been carried out on diamond. Unlike the conventional semiconductors, impurities in diamond are not hydrogenic,<sup>6</sup> and this could affect the MI transition, making studies on diamond very interesting. Previous work on heavily B-doped polycrystalline CVD diamond films<sup>7</sup> suggests that metallic conduction occurs for boron concentrations of the order of  $10^{21} \text{ cm}^{-3}$ . This is greater than early estimates<sup>8</sup> of the critical concentration  $n_c$ , which were predicted to be around  $2 \times 10^{20} \text{ cm}^{-3}$ . Conductivity and Hall effect measurements have been made on the Si:B system,<sup>9</sup> which shows some similarities in electronic structure to boron-doped diamond. (For Si:B,  $n_c$  is  $4 \times 10^{18} \text{ cm}^{-3}$ .)

Diamond is a wide band-gap semiconductor (5.4 eV) and the boron acceptor centers are at 0.37 eV above the valence band. Because of the relatively high energies involved, the temperature range over which localization phenomena may be expected to be observed is comparatively large. In the present work, we have implanted sufficiently high boron concentrations near the surface in a type-IIa natural diamond in order to reach the MI transition in a controlled way. High temperature annealing procedures have been utilized to remove damage produced in the implantation process and to activate the boron dopant.

Very recently metallic samples of boron-doped diamond have been prepared by Ekimov *et al.*<sup>10</sup> using high-pressure, high-temperature growth procedures. Measurements on these samples show that the highly doped diamond becomes a type-II superconductor with a  $T_C$  around 4 K.

Diamonds are classified according to the types of defects that they contain. Unlike type-I diamonds, the type-IIa diamonds contain no deep-lying nitrogen level centers detectable by single-phonon absorption in the infrared spectrum.

Nitrogen centers can act as compensating donors to the implanted boron acceptor centers.<sup>11</sup> High purity type-IIa diamond was used to avoid significant donor compensation due to nitrogen defects.

In this paper, we report on the electrical conductivity, as a function of implanted boron-ion concentration, on both the insulating and just-metallic sides of the transition at temperatures in the range 1.5–300 K. Analysis of the data has been carried out using expressions for the electrical conductivity which apply near the MI transition. Evidence for the occurrence of a MI transition in boron-implanted diamond is presented.

**EXPERIMENTAL**

A high purity, insulating type-IIa diamond specimen, containing less than  $10^{15} \text{ cm}^{-3}$  of impurities, was used in this study. The sample was cut and polished into a rectangular shape of dimensions  $8 \times 3\frac{1}{2} \times 2 \text{ mm}$ . Previous work has shown that implanting with dosages of boron greater than  $\sim 7 \times 10^{15} \text{ ions/cm}^2$  leads to the formation of graphitic regions in the implanted layer. To reach the higher level of doping, a multiple low-energy cold-implantation-rapid-annealing (CIRA) process<sup>12</sup> was used to create a uniform distribution of point defects. The electrical conductivity of the surface layer was measured after each implant of a boron-ion dose of  $3.0 \times 10^{15} \text{ }^+B_{11}/\text{cm}^2$ , spread over the energy range 30–130 keV. Following each implantation step, the sample was annealed at 1200°C for ten minutes under argon. Further conductivity measurements were made as a function of annealing temperature in steps of 100°C from 1200°C to 1700°C. The results presented below refer to samples annealed at 1700°C. The annealing details are discussed below and further details can be found elsewhere.<sup>13,14</sup>

The boron concentration was in the range  $1.0\text{--}4.2 \times 10^{21} \text{ cm}^{-3}$ , corresponding to dosages in the range  $2.1\text{--}8.4 \times 10^{16} \text{ cm}^{-2}$ , and was measured using secondary-ion mass spectroscopy (SIMS) analysis.<sup>15,16</sup> The results of SIMS

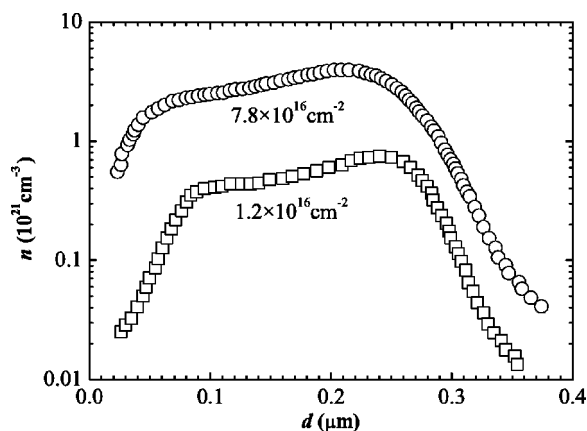


FIG. 1. SIMS results for two boron-ion dosages, showing the boron concentration in diamond versus the depth. The effective thickness of the conducting layer is taken as  $0.2 \mu\text{m}$ .

analysis on two samples are shown in Fig. 1. The thickness of the implanted boron-ion layer was estimated both by SIMS and the TRIM-92 computer simulation program<sup>17</sup> to be about  $0.2 \mu\text{m}$ . The average boron concentration is specified as the total dose divided by this effective thickness. The total implanted dose and SIMS agree closely at lower concentrations and within 10% at concentrations above  $n_c$ . The difference can be attributed to ion-beam current fluctuations during implantation and to the possible loss of some boron ions to the surface or substrate during annealing.

Two-point dc conductivity measurements were performed in a Janis cryostat, equipped with a Lakeshore temperature controller, using a Keithley model 617 programmable electrometer. Sample temperatures in the range 1.5–300 K were measured using a calibrated Lakeshore carbon glass thermometer. The validity of the two-point measurements was checked using four-point technique measurements on some samples. Gold contacts of thickness  $10 \mu\text{m}$ , spaced 5.5 mm apart, were evaporated onto the sample using a vacuum deposition technique. Electrodes were attached by bonding annealed copper leads with silver paint and baking at  $100^\circ\text{C}$  in an oven.

For the conductivity measurements, small input voltages ( $\sim 1$ – $10 \text{ V}$ ) were used. The  $I$ - $V$  curves confirmed ohmic behavior.

## RESULTS AND DISCUSSION

The role of annealing has proved to be important in conductivity studies. We have found a dramatic increase in electrical conductivity when samples were annealed at  $1700^\circ\text{C}$ , compared to those obtained following annealing at lower temperatures. This increase in the conductivity may be related to the removal (or agglomeration) of compensating vacancy centers formed at lower temperatures, or to the diminishing of disorder linked to vacancy related damage induced in the implantation process.

Figure 2 shows the resistance for an implantation dose corresponding to a concentration of  $4.05 \times 10^{21} \text{ cm}^{-3}$  following annealing at five different temperatures. The low-

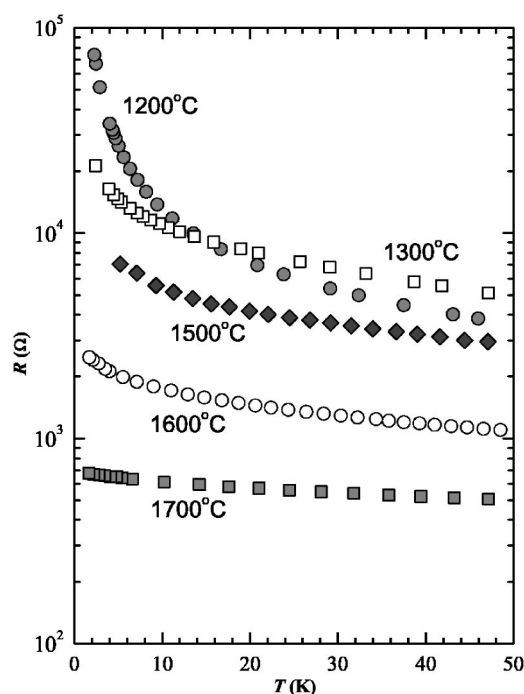


FIG. 2. Electrical resistance  $R$  versus temperature  $T$  for a boron-implanted diamond sample following annealing in argon at temperatures in the range  $1200$  to  $1700^\circ\text{C}$ . The boron concentration in the implanted surface layer is  $4.05 \times 10^{21} \text{ cm}^{-3}$ .

temperature resistance decreases by about two orders of magnitude as the annealing temperature is raised from  $1200$  to  $1700^\circ\text{C}$ . It is not possible to anneal at temperatures higher than  $1700^\circ\text{C}$  without graphitizing the diamond unless high-pressure annealing techniques are used. These were not available for the present experiments. It is not clear what fraction of the implanted boron ions is activated following annealing at  $1700^\circ\text{C}$ , although it is likely to be high. Hall effect measurements, which were made on some samples, confirmed the presence of hole carriers but did not provide a reliable estimate of the carrier concentration because of the decrease in the number of implanted boron atoms very close to the surface. Lower carrier density regions make the largest contributions to the measured Hall voltage. This prevents measurement of the average concentration using this method.

The variation in boron concentration over the *plateau* region of the implanted layer, taken together with the uncertainty in the degree of activation, leads to significant variations in local activated boron concentrations in the implanted layer. In spite of this the main features of the MI transition in this system can be explored using temperature dependent conductivity measurements. The value of the critical concentration  $n_c$  is somewhat uncertain but it is not possible to give a quantitative estimate of the uncertainty.

## INSULATING PHASE

In an insulating phase at sufficiently low temperatures, transport between the distinct localized states in doped semiconductors is described by the well-known hopping law expression<sup>1,2</sup>

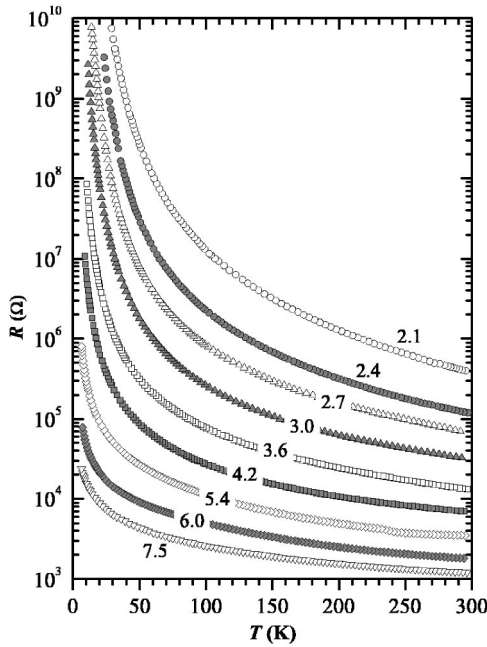


FIG. 3. The boron-ion implanted diamond sample resistance  $R$ , for various dosages, versus the temperature  $T$  in a semilog plot. The dosages are in units of  $10^{16} \text{ cm}^{-2}$ .

$$\sigma(T) = \sigma_m \exp(-[T_0/T]^m), \quad (1)$$

where  $\sigma_m$  is a weakly temperature-dependent factor,  $T_0$  is the characteristic temperature which scales inversely with the localization length  $\xi$ , and  $m$  is the hopping exponent. The variable-range hopping (VRH) regime may be classified as Mott ( $m = \frac{1}{4}$ ) or Efros-Shklovskii (ES) ( $m = \frac{1}{2}$ ), depending on the behavior of the single-particle density of states at the Fermi energy as the temperature is lowered.

Figure 3 shows a plot of the temperature dependence of the resistance  $R$  for implantation dosages in the range  $2.1 \times 10^{16} \text{ cm}^{-2}$  to  $7.5 \times 10^{16} \text{ cm}^{-2}$ . In Fig. 4, the conductivity  $\sigma$  is plotted versus  $T^{-1/2}$  and this shows linear regions at sufficiently low temperatures for the more insulating samples. This is consistent with ES VRH hopping.

Hill and Jonscher<sup>18</sup> and Zabrodskii and Zinov'eva<sup>19</sup> have suggested a method in which the  $\sigma(T)$  ranges of Mott and ES VRH can be identified, and the hopping exponent determined. Their procedure involves plotting the logarithmic derivative of the conductivity as a function of temperature. From Eq. (1) it follows that

$$W = \frac{d \ln \sigma}{d \ln T} = (mT_0^m)T^{-m}. \quad (2)$$

The advantage of this method is that no functional dependence is assumed beforehand, and the hopping exponent can be obtained directly from the slopes of the log  $W$  versus log  $T$  plots, as shown in Fig. 5. This approach also permits the determination of the parameter  $T_0$  in Eq. (1) from the intercepts in these plots.

It becomes increasingly difficult to extract  $T_0$  values from the conductivity data as  $n$  approaches  $n_c$ . The  $W$  versus  $T$  plots develop a region of positive slope, with a maximum

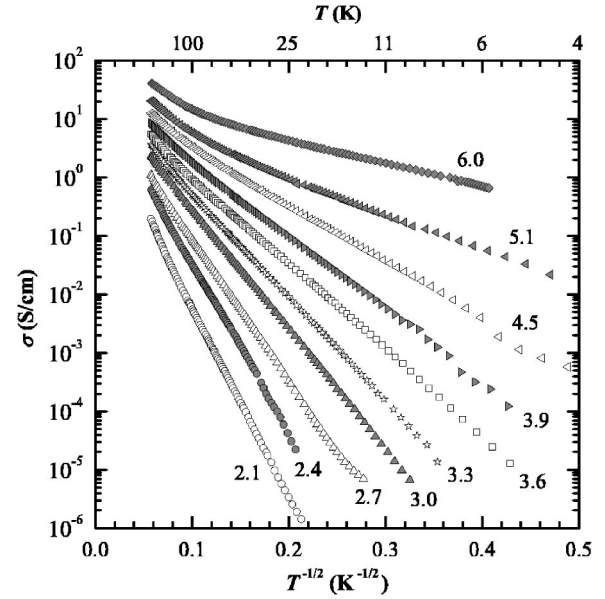


FIG. 4. The lower boron concentration conductivity data for implanted diamond plotted as the conductivity  $\sigma$  versus  $T^{-1/2}$ . The linear form obtained at lower temperatures is consistent with hopping conduction for nonmetallic samples with boron concentrations less than the MI critical concentration, estimated as  $3.9 \times 10^{21} \text{ cm}^{-3}$ . The dosages are in units of  $10^{16} \text{ cm}^{-2}$ .

occurring at finite temperatures. This feature becomes most pronounced close to  $n_c$ , as shown in Fig. 5. Similar behavior has been observed in a number of heavily doped semiconductors and Castner<sup>20</sup> has suggested that thermal excitation

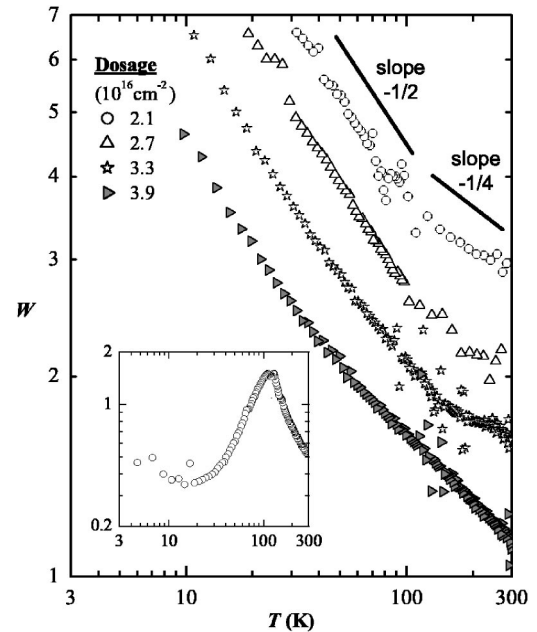


FIG. 5. Logarithmic derivative,  $W$  [defined in Eq. (2)], of the diamond conductivity versus  $T$  for boron concentrations in the range  $1-2 \times 10^{21} \text{ cm}^{-3}$ . The change in slope from  $\frac{1}{4}$  to  $\frac{1}{2}$  as the temperature decreases corresponds to a change from high- $T$  Mott hopping to low- $T$  Efros-Shklovskii hopping. Inset:  $W$  versus  $T$ , for  $n = 3.9 \times 10^{21} \text{ cm}^{-3}$ , showing the maximum discussed in the text.

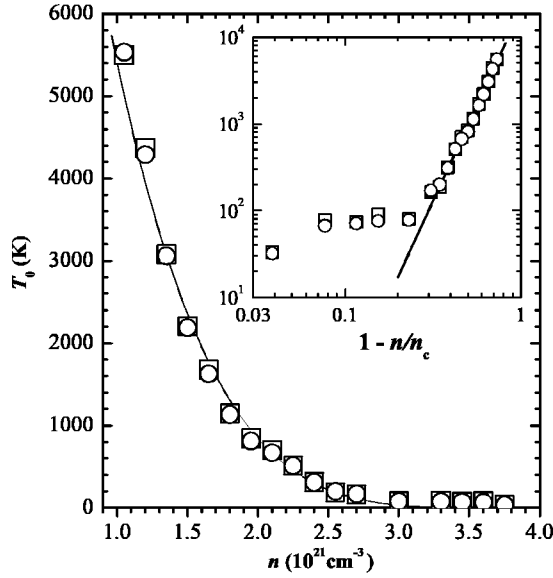


FIG. 6. The ES characteristic temperature  $T_0$ , as a function of the boron concentration  $n$ , in nonmetallic diamond samples. The  $T_0$  values were obtained from Figs. 5 (○) and 4 (□), respectively. It becomes increasingly difficult to extract reliable values of  $T_0$  from the data as  $n \rightarrow n_c$ . Inset: Logarithmic plot of  $T_0$  versus  $(1 - n/n_c)$ , with  $n_c$  taken as  $3.9 \times 10^{21} \text{ cm}^{-3}$ .

of carriers to the mobility edge is responsible for this phenomenon. In this concentration range, it is desirable to make conductivity measurements at lower temperatures in order to obtain reliable values for  $T_0$ . Temperatures below 1.5 K were not available for the present work.

The ES characteristic temperature  $T_0$  for hopping conduction in systems where Coulomb gap effects are important is given by<sup>2</sup>

$$T_0 = \frac{2.8e^2}{4\pi k_B \epsilon_0 \epsilon_r \xi}, \quad (3)$$

with  $\epsilon_r$  the relative permittivity and  $\xi$  the localization length. The behavior of  $\epsilon_r$  and  $\xi$  with concentration for  $n$  approaching  $n_c$  from the insulating side may be expressed in terms of critical exponents as  $\epsilon_r = \epsilon_{r0}(1 - n/n_c)^{-\zeta}$  and  $\xi = \xi_0(1 - n/n_c)^{-\nu}$ . With these forms, Eq. (3) becomes

$$T_0 = \frac{2.8e^2}{4\pi k_B \epsilon_0 \epsilon_{r0} \xi_0} (1 - n/n_c)^\delta = T_0^* (1 - n/n_c)^\delta, \quad (4)$$

with  $\delta = \zeta + \nu$ . The Coulomb gap width  $\Delta_{CG}$  collapses as  $n$  tends towards  $n_c$  corresponding to the divergence of  $\epsilon_r$  and  $\xi$ . The Mott hopping law is obeyed unless  $T$  is sufficiently low so that  $k_B T < \Delta_{CG}$ . The value of  $T_0$  for  $n \ll n_c$  may be estimated using Eq. (3), with  $\epsilon_r = 5.7$ , and  $\xi = 0.3 \text{ nm}$  as the effective Bohr radius of the boron center in diamond.<sup>21</sup> This gives  $T_0^* = 2.7 \times 10^4 \text{ K}$  (2.3 eV), which is much larger than values obtained for many doped semiconductors such as Si:B.<sup>9</sup>

Figure 6 shows a plot of  $T_0$ , obtained from the low  $T$  conductivity data, versus  $n$ . The  $T_0$  values were obtained from the intercepts in Fig. 5, using Eq. (2) with  $m = 1/2$ , and from the slopes in Fig. 4, using Eq. (1). The inset shows a

plot of  $T_0$  versus  $(1 - n/n_c)$ , with  $n_c$  estimated as  $3.9 \times 10^{21} \text{ cm}^{-3}$ . The curve is a fit of Eq. (4), and the fitting constants are  $T_0^* = 2.0 \times 10^4 \text{ K}$  and  $\delta = 4.4$ . This  $T_0^*$  value is comparable with the value of  $2.7 \times 10^4 \text{ K}$  calculated above. The apparent change in slope from the predicted form of Eq. (4), observed in the inset as  $n \rightarrow n_c$ , is expected as  $T_0$  becomes smaller. These data give at best an upper bound to  $T_0$ . In order to obtain more reliable values for  $T_0$ , lower temperatures are required. This feature has also been observed in other systems, such as Si:P.<sup>20,22</sup>

Castner<sup>20</sup> notes that  $\epsilon_r \sim \xi^2$  close to the MI transition, and hence  $\delta = \zeta + \nu \sim 3\nu$ . The result  $\delta = 4.4$  from Fig. 6 therefore implies a localization length exponent  $\nu = 1.5$ . This value is close to the conductivity critical exponent  $\mu = 1.7$ , determined in the next section. Wegner<sup>23</sup> scaling suggests that in three dimensions  $\nu = \mu$ .

A conductivity crossover from Mott to ES hopping is found at relatively high temperatures<sup>24</sup> and a brief account of an analysis of these results, using a scaling method, has been given elsewhere.<sup>25-27</sup> An alternative scaling method has been suggested by Möbius.<sup>28</sup> This method works quite well with our data, consistent with ES hopping being the primary transport mechanism on the insulating side of the MI transition.

Important quantities in the variable range conduction theory are the ratio  $R_{\text{hop}}/\xi$ , where  $R_{\text{hop}}$  is the mean hopping distance, and  $\Delta_{\text{hop}}$  the mean hopping energy difference between localized impurity sites. In the ES VRH case, we have<sup>20</sup>

$$\frac{R_{\text{hop,ES}}(T)}{\xi} = \frac{1}{4} \left( \frac{T_0}{T} \right)^{1/2} \quad (5)$$

and

$$\Delta_{\text{hop,ES}}(T) = \frac{1}{2} k_B T \left( \frac{T_0}{T} \right)^{1/2}. \quad (6)$$

The validity of the ES VRH expressions depends on the condition  $R_{\text{hop}}(T)/\xi > 1$ . Using values for  $T_0$  extracted from the low temperature ES region shows that, in this range, the condition  $R_{\text{hop}}(T) > \xi$  is well satisfied. Furthermore,  $\Delta_{\text{hop,ES}} > k_B T$ , as may be expected.

The ES density of states near the Fermi level in three dimensions may be written as<sup>29</sup>

$$g(E - E_F) = \left( \frac{3^8 \pi^2 \epsilon_r^3 \epsilon_0^3}{2^5 e^6} \right) (E - E_F) = g_0 \cdot (E - E_F). \quad (7)$$

Taking the dielectric constant  $\epsilon_r = 5.7$  for diamond gives for the tunneling exponent  $\alpha (= 1/\xi)$  in SI units as<sup>20</sup>

$$\alpha = \frac{k_B T_0}{10.5} (\pi g_0)^{1/3} = 4.8 \times 10^4 T_0. \quad (8)$$

Using Eq. (5) gives

$$R_{\text{hop,ES}} = 5.2 \times 10^{-6} (T_0 T)^{-1/2}. \quad (9)$$

$T_0$  becomes small close to  $n_c$ , as may be seen from Fig. 6. In this range, at low temperatures, it is possible that  $R_{\text{hop,ES}} \sim t$ , where  $t$  is the doped layer thickness of  $\sim 0.2 \mu\text{m}$ . A

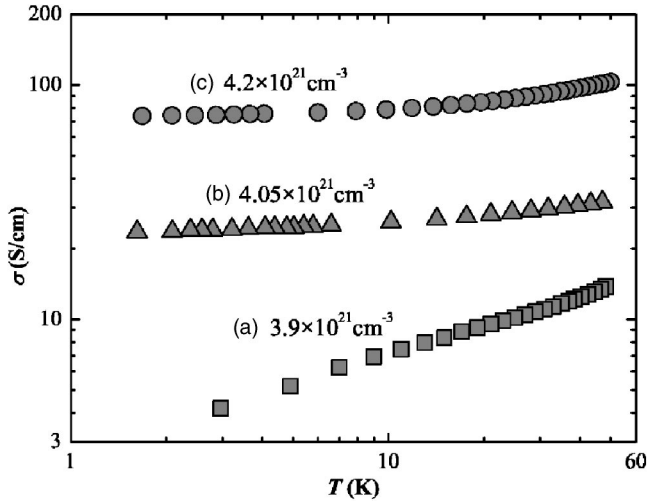


FIG. 7. The conductivity of three boron-implanted diamond samples, indicating metallic-type behavior, versus  $T$ .

dimensional crossover may occur but we have not obtained clear evidence for this.

### METALLIC PHASE

We now report on three samples implanted to total concentrations  $3.9 \times 10^{21} \text{ cm}^{-3}$  (sample A),  $4.05 \times 10^{21} \text{ cm}^{-3}$  (sample B), and  $4.2 \times 10^{21} \text{ cm}^{-3}$  (sample C). The conductivity of these samples is shown in Fig. 7. In order to obtain  $\sigma(0)$ , we use the expression

$$\sigma(T) = \sigma(0) + bT^m \quad (10)$$

and extrapolate to zero temperature. The second term in Eq. (10) is due to quantum corrections to the conductivity related to the electron-electron interaction and has been studied in detail in metallic systems.<sup>1</sup> Many workers have chosen  $m = 1/2$ . However, according to the Al'tshuler-Aronov expression,<sup>30</sup> close to the transition the exponent  $m$  should be  $1/3$ . A value of  $m = 1/3$  was found in Ga:As and in neutron-transmutation-doped Ge:Ga.<sup>31</sup>

Figure 8(a) shows  $\sigma(0)$  versus  $n$  for implantation dosages which are close to the MI transition. The values for  $\sigma(0)$  were obtained by extrapolation using Eq. (10). Justification for using  $m = 1/3$  is indicated in Fig. 8(b), which shows  $\sigma(T)$  plotted against  $T^{1/2}$  and  $T^{1/3}$  for the sample with boron concentration  $3.9 \times 10^{21} \text{ cm}^{-3}$ . It can be seen that the experimental data for sample A agree with the  $T^{1/3}$  form rather than  $T^{1/2}$ . A crossover from  $T^{1/3}$  in the vicinity of the transition to  $T^{1/2}$  with increasing boron concentration is observed, in agreement with theoretical predictions.

Sample A appears to be very close to the MI transition, suggesting  $n_c \approx 3.9 \times 10^{21} \text{ cm}^{-3}$ , consistent with the  $T_0$  versus  $n$  plot. The plot of  $\sigma(0)$  versus  $n$ , shown in Fig. 8(a), then gives the critical exponent  $\mu$  by fitting the scaling relation

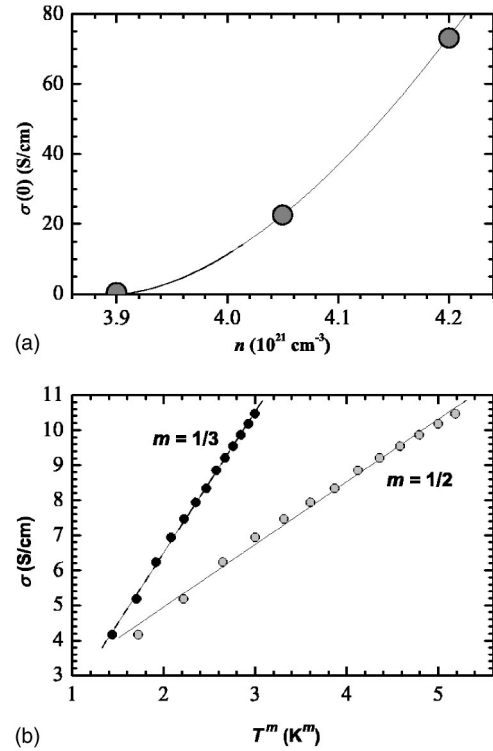


FIG. 8. (a) The estimated  $T=0$  K conductivity, obtained by extrapolation, as a function of boron concentration, for the three highest doped diamond samples. The MI critical concentration is determined as  $n_c \approx 3.9 \times 10^{21} \text{ cm}^{-3}$ . The curve is based on Eq. (11). (b) Conductivity of sample A versus  $T^m$  for  $m=1/2$  and  $m=1/3$ . The value  $m=1/3$  provides a superior linear plot of the data. The exponent  $m=1/3$  is predicted by the Al'tshuler-Aronov expression (Ref. 28) for just-metallic systems.

$$\sigma(0) = \sigma_0 \left( \frac{n - n_c}{n_c} \right)^\mu. \quad (11)$$

We obtain  $\mu \approx 1.7$ , with a large uncertainty because of the small number of points involved and the large extrapolation used in obtaining  $\sigma(0)$ .

Alternative procedures for analyzing conductivity data in the vicinity of  $n_c$  have been proposed by Watanabe *et al.*<sup>31</sup> and Shlimak *et al.*<sup>32</sup> The Watanabe *et al.* method allows for a change in  $m$  in Eq. (10) from  $1/2$  to  $1/3$  as  $n_c$  is approached from the metallic side and is based on the Al'tshuler and Aronov<sup>30</sup> calculation, which gives

$$\sigma(T) = \sigma(0) + c \left( \frac{T}{\sigma(T)} \right)^{1/2}, \quad (12)$$

where  $c$  is a temperature-insensitive constant involving the density of states at the Fermi level. As  $\sigma(0)$  tends to zero, Eq. (12) predicts that  $\sigma(T)$  is proportional to  $T^{1/3}$ . Figure 9 shows a plot of  $\sigma$  versus  $(T/\sigma)^{1/2}$  for the three samples A, B, and C. From this plot, A appears to be just-insulating and B metallic. This implies that  $n_c$  is in the range  $3.9\text{--}4.05 \times 10^{21} \text{ cm}^{-3}$ . Note that, in the case of C, the plot tends to linear form only at the lowest temperatures, while for A and B the points lie on straight lines over a larger range.

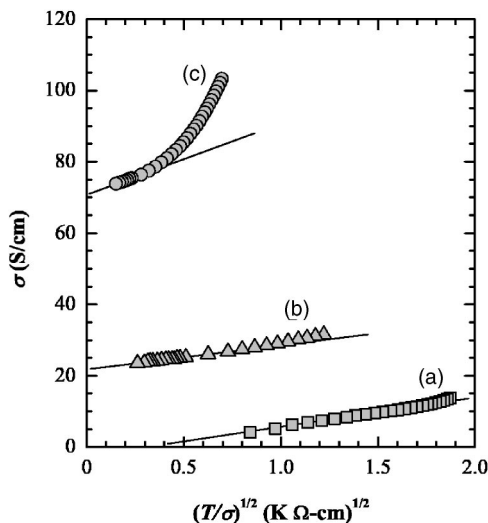


FIG. 9. Electrical conductivity  $\sigma$  versus  $(T/\sigma)^{1/2}$ , as given in Eq. (12) in the text, for boron-implanted diamond with boron concentrations close to the MI critical concentration.

Shlimak *et al.*<sup>32</sup> have suggested that  $n_c$  and  $\mu$  can be obtained without having to extrapolate the conductivity data to zero temperature, provided the slopes of the  $\sigma$  versus  $T$  curves are the same. For the curves to be parallel,  $b$  and  $m$  in Eq. (10) should be the same for different  $n$  values. Using this approach, to find  $n_c$  and  $\mu$ , the relation  $\Delta\sigma(T^*) = \sigma_n(T^*) - \sigma_{n_c}(T^*)$  is applied at any fairly low temperature  $T^*$ . It is claimed that the results obtained for  $\mu$  are quite precise and insensitive to the choice of the temperature  $T^*$  and small variations in  $n_c$ . These claims have been questioned by Sarachik and Bogdanovich,<sup>33</sup> who find that the Shlimak method should be used with caution for Si:B and that extrapolation to  $T=0$  K is preferable.

The Shlimak method produces an exponent of  $\mu \sim 1.8$  using the lowest temperature data. This is consistent with the estimate obtained by extrapolation of the conductivity plots, as described above, and suggests that the Shlimak method may be applicable in diamond.

To characterize the MI transition, Shlimak *et al.*<sup>32</sup> have introduced a parameter  $x$ , given by

$$x = \frac{R(T_1^*)}{R(T_2^*)} \left( \frac{T_1^*}{T_2^*} \right)^{1/3}, \quad (13)$$

with  $R(T_i^*)$  and  $T_i^*$  ( $i=1,2$ ) lying in the region where Eq. (11) is obeyed. Samples with  $x > 1$  demonstrate metallic conductivity, those with  $x < 1$  insulating behavior, while  $x=1$  corresponds to  $n_c$ .

The  $T^{1/3}$  dependence shows that we can place some reliance on Eq. (13) and use it for  $n_c$  determination. Accordingly, we estimate  $x \approx 1$  corresponds to  $n_c = (3.9 \pm 0.5) \times 10^{21} \text{ cm}^{-3}$ , consistent with the previously quoted values.

Using the Mott law  $n_c^{1/3} \cdot a_B^* = 0.25$ , the value obtained for  $n_c$  implies that the mean radius of the boron centers is not

much greater than the lattice spacing of diamond. It is likely that an impurity band is formed at high boron concentrations but further work is needed to confirm this.

The value of the critical exponent is higher than found in many other uncompensated semiconductors, such as Si:P, for which  $\mu = \frac{1}{2}$  has been reported. Our results suggest that boron doped diamond is in a different universality class to other doped semiconductors, such as silicon and germanium.

We have not found evidence for a superconducting transition in our implanted samples. This may be due to the boron concentrations not being sufficiently high or because of residual lattice defects which remain after annealing at  $1700^\circ\text{C}$ . In the recent discovery of superconductivity in high-pressure, high-temperature synthesized boron-doped diamond,<sup>10</sup> boron concentrations approaching  $4.9 \times 10^{21} \text{ cm}^{-3}$  were achieved. It should be possible to achieve these concentrations using implantation methods but it may be necessary to anneal the implanted diamond at high pressures and at temperatures exceeding  $1700^\circ\text{C}$  to remove residual defects.

## CONCLUSION

Using low-temperature electrical conductivity measurements, we have observed the MI transition in surface layers of a heavily ion-implanted natural diamond of high purity. Ion implantation was carried out in multiple steps at low temperature, with annealing between steps and final annealing at  $1700^\circ\text{C}$ .

The critical concentration  $n_c$  is estimated to be  $3.9 \times 10^{21} \text{ cm}^{-3}$  and the conductivity critical exponent  $\mu \approx 1.7$ . There is some uncertainty in the  $n_c$  value as the fraction of implanted boron ions which is activated is not known, although it is expected to be high following the high-temperature annealing. The concentration of boron ions is somewhat dependent on depth below the diamond surface, as revealed by SIMS analysis, even though efforts were made in the implantation process to achieve a homogeneous distribution.

On the metallic side of the transition, the electrical conductivity follows a  $T^m$  law at low temperatures, in agreement with recent work on other semiconductors. For just-metallic samples  $m=1/3$ , tending to  $m=1/2$  at higher concentrations. For  $n < n_c$ , variable range hopping conduction is observed, with a crossover from Efros-Shklovskii to Mott hopping occurring as the temperature is raised.

## ACKNOWLEDGMENTS

Helpful discussions with Dr Boris Aronzon of the Kurchatov Institute, Moscow are gratefully acknowledged. The diamond samples were provided by the De Beers Diamond Research Laboratories. Financial support was obtained from the South African National Research Foundation (NRF) and the University of the Witwatersrand. Further financial assistance was received under the Mellon Foundation Mentoring Scheme.

\*Email address: hoch@magnet.fsu.edu

- <sup>1</sup>N. F. Mott, *Metal-Insulator Transitions*, 2nd ed. (Taylor and Francis, London, 1990).
- <sup>2</sup>B. I. Shklovskii and A. L. Efros, *Electronic Properties of Doped Semiconductors* (Springer-Verlag, Berlin, 1984).
- <sup>3</sup>D. Belitz and T. R. Kirkpatrick, *Rev. Mod. Phys.* **66**, 261 (1994).
- <sup>4</sup>P. P. Edwards, R. L. Johnston, F. Hensel, C. N. R. Rao, and D. P. Tunstall, in *Solid State Physics*, edited by H. Ehrenreich and F. Spaepen (Academic Press, New York, 1999), Vol. 52.
- <sup>5</sup>S. V. Kravchenko and M. P. Sarachik, *Rep. Prog. Phys.* **67**, 1 (2004).
- <sup>6</sup>A. Mainwood, in *Properties and Growth of Diamond*, edited by G. Davies (Inspec, London, 1994).
- <sup>7</sup>M. Werner, O. Dorsch, H. U. Baerwind, L. Haase, W. Seifert, A. Ringhandt, C. Johnston, S. Romani, H. Bishop, and P. R. Chalker, *Appl. Phys. Lett.* **64**, 595 (1994).
- <sup>8</sup>A. W. S. Williams, E. C. Lightowers, and A. T. Collins, *J. Phys. C* **3**, 1727 (1970).
- <sup>9</sup>Peihua Dai, Youzhu Zhang, and M. P. Sarachik, *Phys. Rev. Lett.* **66**, 1914 (1991); **69**, 1804 (1992).
- <sup>10</sup>E. A. Ekimov, V. A. Sidorov, E. D. Bauer, N. N. Mel'nik, N. N. Curro, J. D. Thompson, and M. S. Stishov, *Nature (London)* **428**, 542 (2004).
- <sup>11</sup>*The Properties of Natural and Synthetic Diamond*, edited by J. E. Field (Academic Press, New York, 1992).
- <sup>12</sup>J. F. Prins, *Phys. Rev. B* **38**, 5576 (1988).
- <sup>13</sup>J. F. Prins, *Mater. Sci. Rep.* **7**, 271 (1992).
- <sup>14</sup>J. F. Prins, *Nucl. Instrum. Methods Phys. Res. B* **59/60**, 1387 (1991).
- <sup>15</sup>T. Tshepe, J. F. Prins, and M. J. R. Hoch, *Diamond Relat. Mater.* **8**, 1508 (1999).
- <sup>16</sup>The boron SIMS analysis was carried out by Charles Evans and Associates, California, 1999.
- <sup>17</sup>J. F. Ziegler, J. P. Biersack, and U. Littmark, *The Stopping and Range of Ions in Solids* (Pergamon, New York, 1985).
- <sup>18</sup>R. Hill and A. K. Jonscher, *J. Non-Cryst. Solids* **32**, 53 (1979).
- <sup>19</sup>A. G. Zabrodskii and K. N. Zinov'eva, *Sov. Phys. JETP* **59**, 425 (1984).
- <sup>20</sup>T. G. Castner, in *Hopping Transport in Solids*, edited by M. Polak and B. I. Shklovskii (Elsevier/North-Holland, Amsterdam, 1991), Vol. 1.
- <sup>21</sup>A. T. Collins, *The Physics of Diamond* (IOS Press, Amsterdam, 1997).
- <sup>22</sup>M. Hornung and H. v. Löhneysen, *Czech. J. Phys.* **46**, 2437 (1996).
- <sup>23</sup>F. J. Wegner, *Z. Phys. B* **35**, 207 (1979).
- <sup>24</sup>T. Sato, K. Ohashi, H. Sugai, T. Sumi, K. Haruna, H. Maeta, N. Matsumoto, and H. Otsuka, *Phys. Rev. B* **61**, 12970 (2000).
- <sup>25</sup>A. Aharony, Y. Zhang, and M. P. Sarachik, *Phys. Rev. Lett.* **68**, 3900 (1992).
- <sup>26</sup>Y. Meir, *Phys. Rev. Lett.* **77**, 5265 (1996).
- <sup>27</sup>M. J. R. Hoch, T. Tshepe, and J. F. Prins, *Ann. Phys. (N.Y.)* **8**, SI-93 (1999).
- <sup>28</sup>A. Möbius, *J. Phys. C* **18**, 4639 (1985).
- <sup>29</sup>C. J. Adkins, *J. Phys.: Condens. Matter* **1**, 1253 (1989).
- <sup>30</sup>B. L. Al'tshuler and A. G. Aronov, *Pis'ma Zh. Eksp. Teor. Fiz.* **37**, 349 (1983); [*JETP Lett.* **37**, 410 (1983)].
- <sup>31</sup>M. Watanabe, Y. Ootuka, K. M. Itoh, and E. E. Haller, *Phys. Rev. B* **58**, 9851 (1998).
- <sup>32</sup>I. Shlimak, M. Kaveh, R. Ussyshkin, V. Ginodman, and L. Resnick, *Phys. Rev. Lett.* **77**, 1103 (1996).
- <sup>33</sup>M. P. Sarachik and S. Bogdanovich, *Phys. Rev. Lett.* **78**, 3977 (1997).